Electronic Supplementary Material (ESI) for Dalton Transactions.
This journal is © The Royal Society of Chemistry 2020

Luminescent Polypyridyl Heteroleptic Cr^{III} Complexes with High Quantum Yields and Long Excited State Lifetimes

Juan-Ramón Jiménez,* Maxime Poncet, Benjamin Doistau, Céline Besnard and Claude Piguet*

Supporting Information

(37 pages)

Appendix 1. Experimental section.

Solvents and starting materials

Reagent grade acetonitrile (ACN) was distilled from CaH_2. All other chemicals such as $CrCl_3 \cdot 3THF$, $AgCF_3SO_3$, (n-Bu_4)NPF_6 and organic solvents were purchased from commercial suppliers and used without further purification. The ligand ddpd, dqp and dqpOMe were prepared according to published methods.[S1-S2]

Preparation of [Cr(dqp)Cl_3]. The ligand dqp (250 mg, 0.75 mmol) was added into a solution of $CrCl_3 \cdot 3THF$ (280 mg, 0.75 mmol) in propan-2-ol (15 mL). The resulting green solution was heated in a microwave to 160°C during 4 h. The mixture was filtered and the green solid was washed with warm ethanol (2 x 10 mL), dichloromethane (20 mL) and diethyl ether (2 x 20 mL). The product was dried under vacuum to obtain a crystalline green powder [Cr(dqp)Cl_3] (yield 90%). Slow diffusion of diethyl ether into a concentrated solution of the complex in *N*,*N*'-dimethylformamide led to the formation of green crystals suitable for X-ray diffraction. Elemental analysis: Calcd for: $C_{23}H_{15}Cl_3CrN_3 \cdot 0.1H_2O \cdot 0.3CH_2Cl_2$ C, 53.9; H, 3.42; N, 8.09. Found C, 53.8; H, 3.47; N, 8.11.

Preparation of [Cr(dqp)(SO_3CF_3)$_3$]. A mixture of [Cr(dqp)Cl_3] (50 mg, 0.09 mmol) and silver triflate (83 mg, 0.32 mmol) in distilled acetonitrile (1 mL), was heated under microwave irradiation in a sealed cap at 140°C during 30 min. After cooling to room temperature, the resulting red solution was filtered to remove the AgCl generated during the reaction. ESI-MS (CH_3CN) *m/z*: $[Cr(dqp)(OSO_2CF_3)_2]^+$ calc: 682.9, found: 682.9 (Figure S1). This solution was used directly for the next step.

Preparation of [Cr(dqp)(tpy)](PF_6) (1). A red solution of [Cr(dqp)(OSO_2CF_3)$_3$] in distilled acetonitrile was loaded into a 5 ml MW vial containing 1 equivalent of the tpy ligand in 1 mL of CH_3CN. The solution was heated under microwave irradiation for 12h at 70°C. After cooling to room temperature, the solvent was removed under reduced pressure yielding an orange residue. The orange residue was dissolved in methanol (2 mL) and few drops of a saturated methanol solution of (n-Bu_4)NPF_6 were added. The yellow precipitate was filtered and washed with cold MeOH (1 x 5 mL), dichloromethane (20 mL) and diethyl ether (2 x 15 mL) to give [Cr(dqp)(tpy)](PF_6)$_3$ (yield 40%) as a fine yellow powder. Slow diffusion of diethyl ether into a concentrated solution of the complex in acetonitrile led to the formation of orange crystals suitable for XRD. Elemental Analysis: Calcd for $C_{38}H_{26}CrF_{18}N_6P_3 \cdot 2.2CH_2Cl_2 1.3CH_3CN$: C, 39.73; H, 2.67; N, 7.9 found C, 39.72; H, 2.68; N, 7.90.

Preparation of [Cr(dqp)(L)](CF_3SO_3)$_3$ (L = ddpd (2) dqpOMe (3)). A red solution of [Cr(dqp)(OSO_2CF_3)$_3$] in distilled acetonitrile was loaded into a 5 ml MW vial containing 1 equivalent of ddpd or dqpOMe in 1 mL distilled acetonitrile. The solution was heated under microwave irradiation for 6h at 120°C and 140°C respectively. After cooling to room temperature, acetonitrile was added and the mixture filtered to remove impurities. The solvent was then removed under reduced pressure yielding an orange residue. The orange residue was dissolved in water, filtered, evaporated again and dried under vacuum to give [Cr(ddpd)(dqp)]($CF_3SO_3CF_3$)$_3$ (yield 60%) and[Cr(dqp)(dqpOme)](CF_3SO_3)$_3$ (yield

80%). The orange residue was dissolved in acetonitrile and precipitate slowly with diethyl ether to give in both cases an orange/yellow precipitate which was washed with cold MeOH (1 x 5 mL), dichloromethane (20 mL) and diethyl ether (2 x 15 mL). Slow diffusion of diethyl ether into a concentrated solutions of the complexes in acetonitrile led to the formation of orange crystals suitable for XRD. ESI-MS (CH_3CN) *m/z*: $[Cr(ddpd)(dqp)](CF_3SO_3)_2]^+$ calc: 945.9, found: 946.0. Elemental analysis: Calcd $C_{53}H_{40}CrF_9N_6O_{10}S_3 \cdot 0.9CH_2Cl_2 \cdot 0.35CH_3CN$: C, 49.27; H, 3.25 N, 6.68 found C, 49.14; H, 2.99; N, 6.94. ESI-MS (CH_3CN) *m/z*: $[Cr(dqp)(dqpOe)](CF_3SO_3)_2]^+$ calc: 1046., found: 1046.1. Elemental analysis: Calcd $C_{43}H_{32}CrF_9N_8O_9S_3 \cdot 1.3H_2O$: C, 45.01; H, 3.04 N, 9.77 found C, 45.01; H, 3.05; N, 9.75.

Spectroscopic and analytical measurements.

Pneumatically-assisted electrospray (ESI) mass spectrum was recorded from 10^{-4} M solution on an Applied Biosystems API 150EX LC/MS System equipped with a Turbo Ionspray source®. Elemental analyses were performed by K. L. Buchwalder from the Microchemical Laboratory of the University of Geneva. Absorption spectra in water solution were recorded using a Lambda 1050 Perkin Elmer spectrometer (quartz cell path length 1 cm or 1 mm, 290-800 nm domain, 2×10^{-4} mol/L and 650-800 nm domain). Emission spectra (excitation at 355 nm) was recorded from either room temperature or frozen solution samples (for frozen solutions: CH_3CN/propionitrile 6/4 at C ≈ 5×10^{-3} mol/L), or freeze-pump-thaw degassed acetonitrile solution (C ≈ 10^{-4} mol/L) for room temperature solutions 293 K, with a Fluorolog (Horiba Jobin-Yvon), equipped with iHR320, a Xenon lamp 450 Watt Illuminator (FL-1039A/40A) and a water-cooled photo multiplier tube (PMT Hamamatsu R2658 or R928), and corrected for the spectral response of the system. The emission spectra were recorded as a function of the wavelength and transformed into wavenumbers.[S3] For time-resolved experiments, the decay curves were recorded from previously excited samples at 77K and 293K, with a photomultiplier (Hamamatsu R2658 or R928) and a digital oscilloscope (Tektronix MDO4104C). Pulsed excitation at 355 nm was obtained with the third harmonic of a pulsed Nd:YAG laser (Quantel Qsmart 850). Low temperature (77 K) was achieved using liquid quartz transparent Deward filled with liquid N_2 in the centre of which samples were placed. Samples solutions (CH_3CN/propionitrile) 6/4 at C ≈ 5×10^{-3} mol/L), were introduced in quartz tube (4 mm interior diameter) and introduced into the sample holder of the Dewar. The oxygen free decay curve measurements were recorded at 293 K for acetonitrile solutions of the complex (C ≈ 10^{-5} mol/L). Aerated solutions were prepared by using no-degassed water as solvent. All emission quantum yields were measured according to the relative method using the reported $[Cr(ddpd)_2]^{3+}$ (Φ_{Cr}^{L} =12.1%; λ_{exc} = 435 nm). The measurement was carried out by following the previously reported method (IUPAC Technical Report).[S4] The measurements were achieved in CH_3CN, at room temperature and λ_{exc} = 435 nm (manifold $Cr(^4T_2 \leftarrow {}^4A_2)$/LMCT). Molar concentrations were adjusted to $1\text{x}10^{-5}$ M.

X-Ray Crystallography.

Summary of crystal data, intensity measurements and structure refinements for *rac*-[Cr(dqp)(tpy)]$(PF_6)_3$, *rac*-[Cr(ddpd)(dqp)]$(CF_3SO_3)_3$ and *rac*-[Cr(dqp)(dqpOMe)]$(CF_3SO_3)_3$ compound were collected in Tables S1-S12 (ESI). The crystals were mounted on MiTeGen cryoloops with protection oil. X-ray data collections were performed with an Agilent SuperNova Dual diffractometer equipped with a CCD Atlas detector (Cu[Kα] radiation) or a Rigaku symergy S equipped with an hypix detector. The structures were solved in SHELXT by using dual space methods.[S5] Full-matrix least-square refinements on F^2 were performed with SHELXL[S6] within the Olex2 program.[S7] CCDC 2015187-2015190 contain the supplementary crystallographic data. The cif files can be obtained free of charge on www.ccdc.cam.ac.uk.

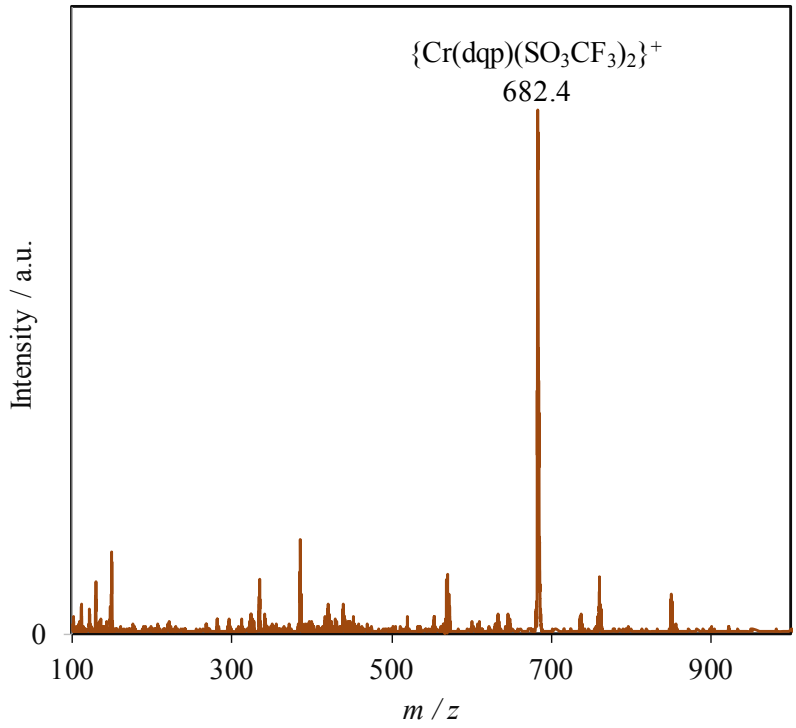

Figure S1. ESI-MS spectra recorded upon reaction of [Cr(dqp)Cl_3] with $AgCF_3SO_3$

Table S1. Crystal data and structure refinement for *rac*-[Cr(dqp)Cl_3]

Empirical formula	$C_{23}H_{15}Cl_3CrN_3$
Formula weight	491.73
Temperature/K	150(2)
Crystal system	monoclinic
Space group	C2/c
a/Å	12.5368(2)
b/Å	12.0583(2)
c/Å	13.3923(2)
α/°	90
β/°	103.770(2)
γ/°	90
Volume/Å^3	1966.36(6)
Z	4
ρ_{calc}g/cm^3	1.661
μ/mm^{-1}	8.669
F(000)	996.0
Crystal size/mm^3	0.229 × 0.156 × 0.126
Radiation	CuKα (λ = 1.54184)
2Θ range for data collection/°	10.324 to 148.778
Index ranges	-15 ≤ h ≤ 15, -15 ≤ k ≤ 14, -16 ≤ l ≤ 16
Reflections collected	29407
Independent reflections	2005 [R_{int} = 0.0284, R_{sigma} = 0.0088]
Data/restraints/parameters	2005/0/138
Goodness-of-fit on F^2	1.074
Final R indexes [I>=2σ (I)]	R_1 = 0.0230, wR_2 = 0.0686
Final R indexes [all data]	R_1 = 0.0232, wR_2 = 0.0688
Largest diff. peak/hole / e Å^{-3}	0.32/-0.41

Table S2. Selected bond distances (Å), bond angles (°) in *rac*-[Cr(dqp)Cl_3]

Atom	Atom	Length/Å
Cr1	Cl1	2.3559(5)
Cr1	Cl2*	2.3251(3)
Cr1	Cl2	2.3250(3)
Cr1	N1*	2.0770(13)
Cr1	N1	2.0770(13)
Cr1	N2	2.0587(17)

Atom	Atom	Atom	Angle/°
Cl2*	Cr1	Cl1	89.108(10)
Cl2	Cr1	Cl1	89.107(10)
Cl2	Cr1	Cl2*	178.21(2)
N1	Cr1	Cl1	93.09(3)
N1*	Cr1	Cl1	93.09(3)
N1*	Cr1	Cl2	91.51(4)
N1	Cr1	Cl2	88.59(4)
N1*	Cr1	Cl2*	88.58(4)
N1	Cr1	Cl2*	91.51(4)
N1	Cr1	N1*	173.81(7)
N2	Cr1	Cl1	180
N2	Cr1	Cl2	90.893(10)
N2	Cr1	Cl2*	90.892(10)
N2	Cr1	N1*	86.91(3)
N2	Cr1	N1	86.91(3)

Table S3. Interplanar angles (°) in *rac*-[Cr(dqp)Cl_3]

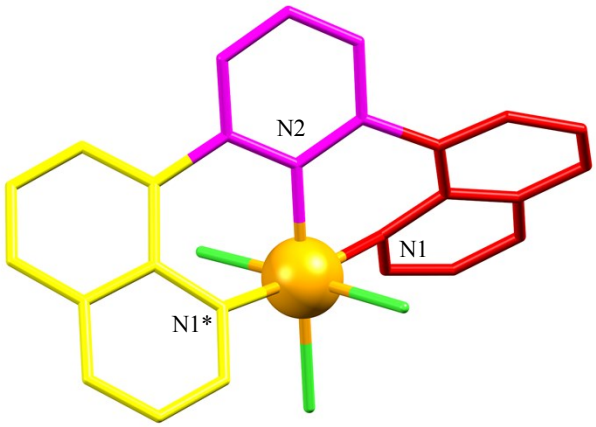

Plane	mean deviation in Å	max deviation in Å (atom)
QUIN1 N1 C5 C9 C8 C7 C6 C4 C3 C2 C1	0.086	0.146 (C9)
PYR1N2 C10 C11 C12 C11 C10	0.001	0.002 (C11)

Interplanar angles (°)

	PYR1	QUIN1*
QUIN1	38.9	77.8
PYR1		38.9

QUIN1* is obtained from QUIN1 by applying the symmetry operation (1-X,Y,3/2-Z)

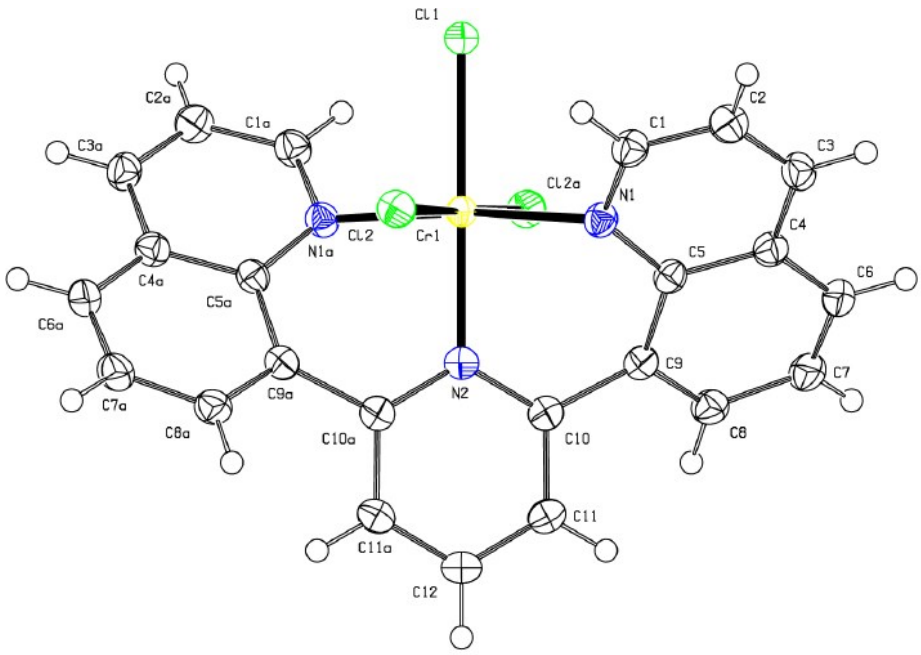

Figure S2 ORTEP view of $[Cr(dqp)Cl_3](PF_6)_3$ (**1**) with numbering scheme. Thermal ellipsoids are drawn at 50% probability level.

Table S4. Crystal data and structure refinement for *rac*-[Cr(dqp)(tpy)]$(PF_6)_3$.

Empirical formula	$C_{42.17}H_{32}CrF_{17.48}N_8O_{0.52}P_{2.83}S_{0.17}$
Formula weight	1136.37
Temperature/K	149.99(10)
Crystal system	orthorhombic
Space group	Pbca
a/Å	17.10349(6)
b/Å	17.98863(8)
c/Å	28.79512(12)
α/°	90
β/°	90
γ/°	90
Volume/Å^3	8859.35(6)
Z	8
ρ_{calc}g/cm^3	1.704
μ/mm^{-1}	4.261
F(000)	4574.0
Crystal size/mm^3	0.319 × 0.243 × 0.189
Radiation	Cu Kα (λ = 1.54184)
2Θ range for data collection/°	6.138 to 148.854
Index ranges	$-21 \leq h \leq 18$, $-22 \leq k \leq 20$, $-35 \leq l \leq 35$
Reflections collected	95378
Independent reflections	8997 [R_{int} = 0.0245, R_{sigma} = 0.0096]
Data/restraints/parameters	8997/137/712
Goodness-of-fit on F^2	1.040
Final R indexes [I>=2σ (I)]	R_1 = 0.0452, wR_2 = 0.1200
Final R indexes [all data]	R_1 = 0.0459, wR_2 = 0.1206
Largest diff. peak/hole / e Å^{-3}	1.59/-0.75

Table S5. Selected bond distances (Å), bond angles (°) in *rac*-[Cr(dqp)(tpy)]$(PF_6)_3$.

Atom	Atom	Length/Å
Cr1	N2 (dqp)	2.0272(18)
Cr1	N1 (dqp)	2.0611(18)
Cr1	N5 (tpy)	1.9894(19)
Cr1	N6 (tpy)	2.0685(18)
Cr1	N4 (tpy)	2.0832(18)
Cr1	N3 (dqp)	2.0725(19)

Atom	Atom	Atom	Angle/°
N2	Cr1	N1	88.57(7)
N2	Cr1	N6	97.09(7)
N2	Cr1	N4	106.21(7)
N2	Cr1	N3	90.60(7)
N1	Cr1	N6	93.35(7)
N1	Cr1	N4	89.70(7)
N1	Cr1	N3	176.04(7)
N5	Cr1	N2	175.35(7)
N5	Cr1	N1	90.84(7)
N5	Cr1	N6	78.33(7)
N5	Cr1	N4	78.41(8)
N5	Cr1	N3	90.29(8)
N6	Cr1	N4	156.58(7)
N6	Cr1	N3	90.59(7)
N3	Cr1	N4	86.81(7)

Table S6. Interplanar angles (°) in *rac*-[Cr(dqp)(tpy)]$(PF_6)_3$

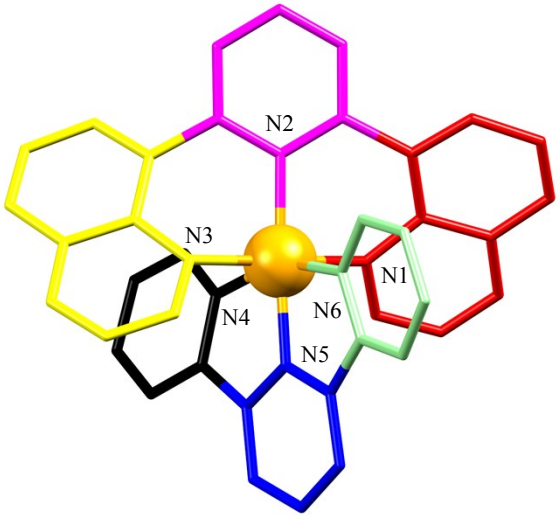

Plane	mean deviation in Å	max deviation in Å (atom)
QUIN1 N1 C1 C2 C3 C4 C5 C9 C8 C7 C6	0.078	0.137 (C9)
PYR1 N2 C10 C11 C12 C13 C14	0.021	0.030 (C14)
QUIN2 N3 C23 C22 C21 C19 C20 C15 C16 C17 C18	0.069	0.125 (N3)
PYR2 N4 C28 C27 C26 C25 C24	0.016	0.024 (N4)
PYR3 C29 C30 C31 C32 C33 N5	0.014	0.020 (N5)
PYR4 N6 C34 C35 C36 C37 C38	0.006	0.010 (N6)

Interplanar Angles (°)

	PYR1	QUIN2	PYR2	PYR3	PYR4
QUIN1	27.6	71.8	69.1	59.8	64.4
PYR1		44.3	53.9	50.7	59.4
QUIN2			44.2	53.7	63.2
PYR2				13.6	20.1
PYR3					10.2

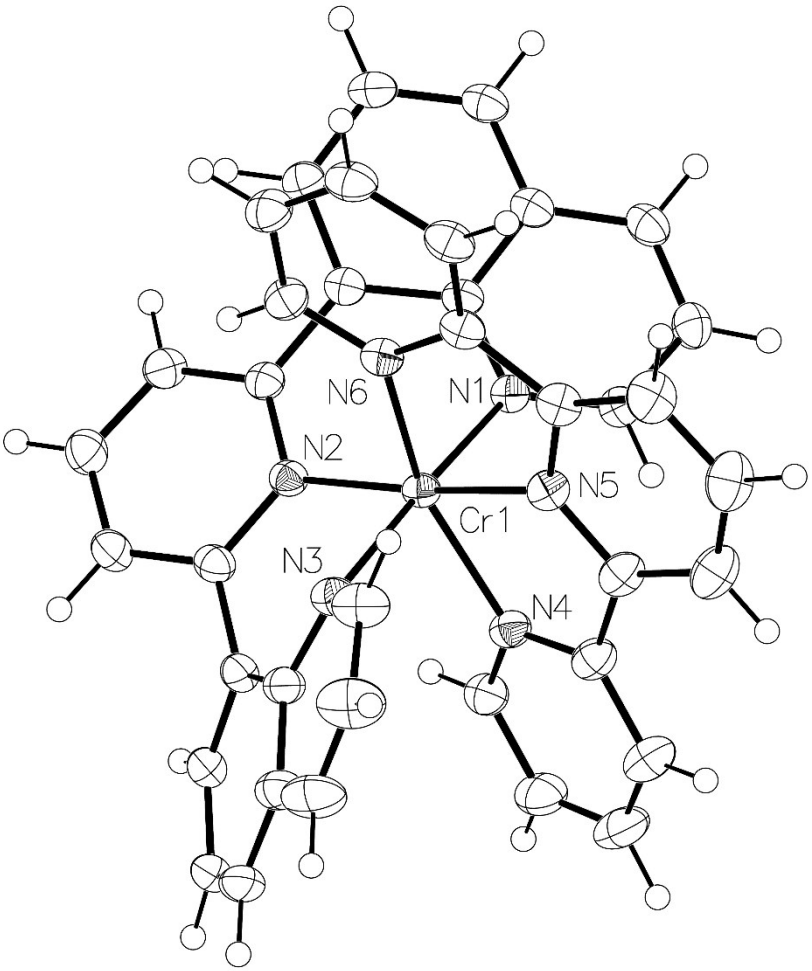

Figure S3 ORTEP view of $[Cr(dqp)(tpy)](PF_6)_3$ (**1**) with numbering scheme. Thermal ellipsoids are drawn at 50% probability level. Counter ions are omitted for clarity.

Table S7. Crystal data and structure refinement for *rac*-[Cr(ddpd)(dqp)]$(CF_3SO_3)_3$

Empirical formula	$C_{44}H_{38}CrF_{18}N_{10}P_3$
Formula weight	1193.75
Temperature/K	149.99(10)
Crystal system	monoclinic
Space group	$P2_1/c$
a/Å	21.14124(15)
b/Å	22.83951(17)
c/Å	20.55852(15)
α/°	90
β/°	90.3997(7)
γ/°	90
Volume/Å^3	9926.55(12)
Z	8
ρ_{calc}g/cm^3	1.598
μ/mm^{-1}	3.837
F(000)	4824.0
Crystal size/mm^3	0.637 × 0.394 × 0.037
Radiation	Cu Kα (λ = 1.54184)
2Θ range for data collection/°	4.18 to 147.57
Index ranges	$-25 \leq h \leq 25$, $-27 \leq k \leq 25$, $-24 \leq l \leq 24$
Reflections collected	87579
Independent reflections	18950 [R_{int} = 0.0541, R_{sigma} = 0.0346]
Data/restraints/parameters	18950/0/1377
Goodness-of-fit on F^2	1.065
Final R indexes [I>=2σ (I)]	R_1 = 0.0542, wR_2 = 0.1505
Final R indexes [all data]	R_1 = 0.0659, wR_2 = 0.1579

Table S8. Interplanar angles (°) in *rac*-[Cr(ddpd)(dqp)]$(CF_3SO_3)_3$

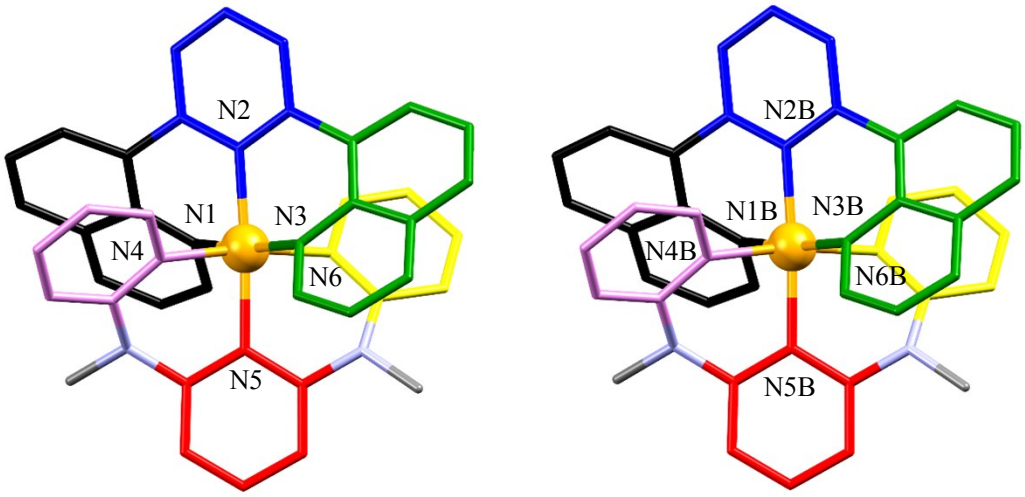

Plane	mean deviation in Å	max deviation in Å (atom)
N1 C1 C2 C3 C4 C5 C9 C8 C7 C6 ***quin1***	0.077	0.136 (N1)
N1B C1B C2B C3B C4B C5B C9B C8B C7B C6B	0.090	0.153 (C9B)
N2 C14 C13 C12 C11 C10 ***pyr1***	0.011	0.016 (C14)
N2B C14B C13B C12B C11B C10B	0.006	0.008 (C13B)
N3 C23 C22 C21 C19 C20 C15 C16 C17 C18 ***quin2***	0.073	0.137 (N3)
C15B C16B C17B C18B C19B C21B C22B C23B N3B C20B	0.065	0.123 (N3B)
N4 C24 C25 C26 C27 C28 ***pyr2***	0.022	0.035 (N4)
N4B C28B C27B C26B C25B C24B	0.019	0.030 (N4B)
N5 C34 C33 C32 C31 C30 ***pyr3***	0.04	0.005 (C34)
N5B C30B C31B C32B C33B C34B	0.004	0.005 (N5B)
N6 C36 C37 C38 C39 C40 ***pyr4***	0.026	0.039 (N6)
N6B C40B C39B C37B C38B C36B	0.023	0.037 (N6B)

Angles between least-square planes (in ˚). Two complexes are present in the asymmetric unit. Values for the second molecule are given in blue

	Pyr1	Quin2	Pyr2	Pyr3	Pyr4
Quin1	36.7	74.7	32.0	41.6	84.2
	38.3	77.0	31.4	46.1	85.9
Pyr1		38.1	53.5	22.0	53.1
		38.8	52.8	20.3	54.1
Quin2			83.8	42.1	27.7
			84.9	39.2	31.6
Pyr2				41.6	77.9
				45.7	76.7
Pyr3					42.9
					39.9

Table S9. Selected bond distances (Å), bond angles (°) in *rac*-[Cr(ddpd)(dqp)]$(CF_3SO_3)_3$

Atom	Atom	Length/Å
Cr1	N1	2.052(2)
Cr1	N2	2.032(2)
Cr1	N3	2.051(2)
Cr1	N4	2.050(2)
Cr1	N5	2.041(2)
Cr1	N6	2.042(2)

Atom	Atom	Atom	Angle/°
N2	Cr1	N1	88.27(9)
N2	Cr1	N3	87.66(9)
N2	Cr1	N4	93.04(9)
N2	Cr1	N5	179.60(10)
N2	Cr1	N6	93.68(9)
N3	Cr1	N1	175.48(10)
N4	Cr1	N1	93.69(9)
N4	Cr1	N3	88.49(9)
N5	Cr1	N1	91.37(10)
N5	Cr1	N3	92.71(10)
N5	Cr1	N4	86.83(9)
N5	Cr1	N6	86.46(10)
N6	Cr1	N1	87.42(10)
N6	Cr1	N3	90.88(9)
N6	Cr1	N4	173.22(9)

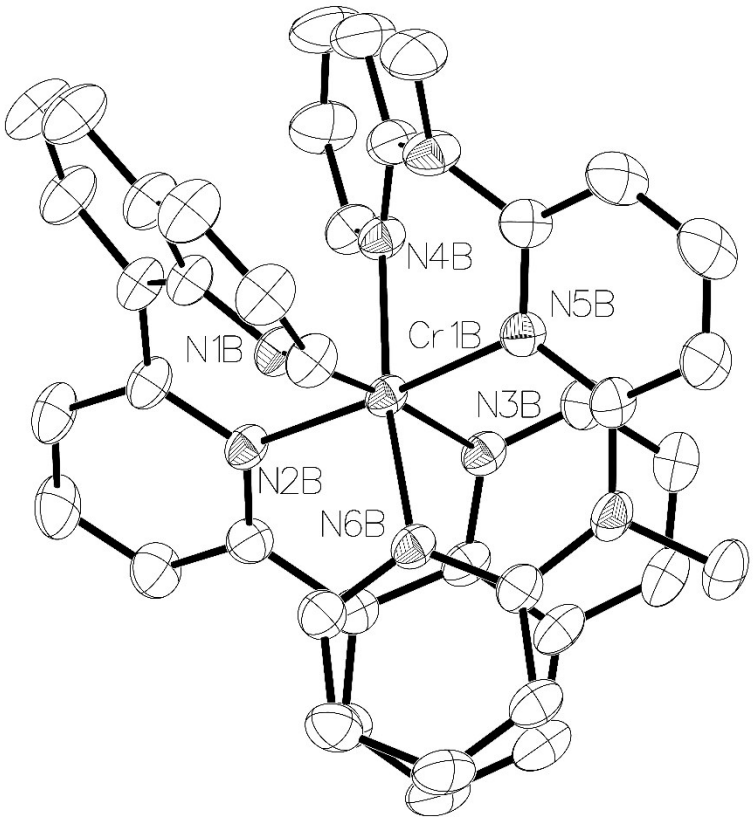

Figure S4 ORTEP view of $[Cr(ddpd)(dqp)](CF_3SO_3)_3$ (**2**) with numbering scheme. Thermal ellipsoids are drawn at 50% probability level. Counter ions and H atoms are omitted for clarity.

Table S10. Crystal data and structure refinement for *rac*-[Cr(dqp)(dqpOMe)]$(CF_3SO_3)_3$

Empirical formula	$C_{52}H_{35}CrF_9N_7O_{10}S_3$
Formula weight	1237.05
Temperature/K	150.01(10)
Crystal system	triclinic
Space group	P-1
a/Å	13.1076(5)
b/Å	13.8460(5)
c/Å	14.7792(5)
α/°	100.865(3)
β/°	90.278(3)
γ/°	108.118(3)
Volume/Å^3	2497.76(16)
Z	2
ρ_{calc}g/cm^3	1.645
μ/mm^{-1}	3.975
F(000)	1258.0
Crystal size/mm^3	0.522 × 0.286 × 0.164
Radiation	Cu Kα (λ = 1.54184)
2Θ range for data collection/°	6.104 to 141.146
Index ranges	$-15 \leq h \leq 15$, $-16 \leq k \leq 16$, $-13 \leq l \leq 18$
Reflections collected	18796
Independent reflections	9338 [R_{int} = 0.0199, R_{sigma} = 0.0215]
Data/restraints/parameters	9338/0/742
Goodness-of-fit on F^2	1.041
Final R indexes [I>=2σ (I)]	R_1 = 0.0500, wR_2 = 0.1271
Final R indexes [all data]	R_1 = 0.0516, wR_2 = 0.1283
Largest diff. peak/hole / e Å^{-3}	1.85/-0.78

Table S11. Selected bond distances (Å), bond angles (°) in *rac*-[Cr(dqp)(dqpOMe)]$(CF_3SO_3)_3$

Atom	Atom	Length/Å
Cr1	N1	2.060(2)
Cr1	N2	2.054(2)
Cr1	N3	2.067(2)
Cr1	N4	2.070(2)
Cr1	N5	2.038(2)
Cr1	N6	2.058(2)

Atom	Atom	Atom	Angle/°
N1	Cr1	N3	174.47(9)
N1	Cr1	N4	92.67(8)
N2	Cr1	N1	87.01(8)
N2	Cr1	N3	87.47(9)
N2	Cr1	N4	92.20(9)
N2	Cr1	N6	94.02(8)
N3	Cr1	N4	87.96(9)
N5	Cr1	N1	92.23(8)
N5	Cr1	N2	178.29(8)
N5	Cr1	N3	93.30(9)
N5	Cr1	N4	86.31(9)
N5	Cr1	N6	87.48(8)
N6	Cr1	N1	88.34(8)
N6	Cr1	N3	91.64(9)
N6	Cr1	N4	173.74(9)

Table S12. Interplanar angles (°) in *rac*-[Cr(dqp)(dqpOMe)]$(CF_3SO_3)_3$

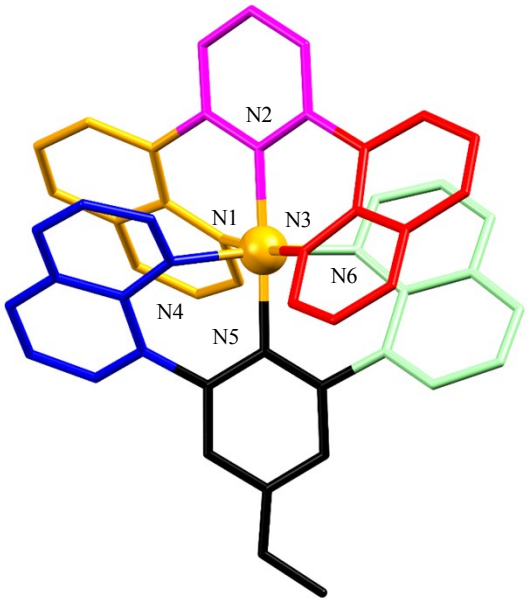

Plane	mean deviation in Å	max deviation in Å (atom)
QUIN1 N1 C1 C2 C3 C4 C9 C8 C7 C6 C5	0.105	0.170 (N1)
PYR1 N2 C14 C13 C12 C11 C10	0.002	0.004 (C11)
QUIN2 C15 C16 C17 C18 C19 C20 C21 C22 N3 C23	0.085	0.142 (N3)
QUIN3 N4 C24 C25 C26 C27 C29 C30 C31 C32 C28	0.092	0.162 (N4)
PYR2 N5 C33 C34 C35 C38 C39	0.009	0.013 (C35)
QUIN4 N6 C48 C40 C41 C42 C43 C44 C45 C46 C47	0.092	0.157 (C40)

Interplanar angle (°)

	PYR1	QUIN2	QUIN3	PYR2	QUIN4
QUIN1	40.1	79.4	11.8	41.5	83.3
PYR1		39.5	41.6	17.1	45.5
QUIN2			80.6	45.6	20.9
QUIN3				37.6	80.1
PYR2					42.6

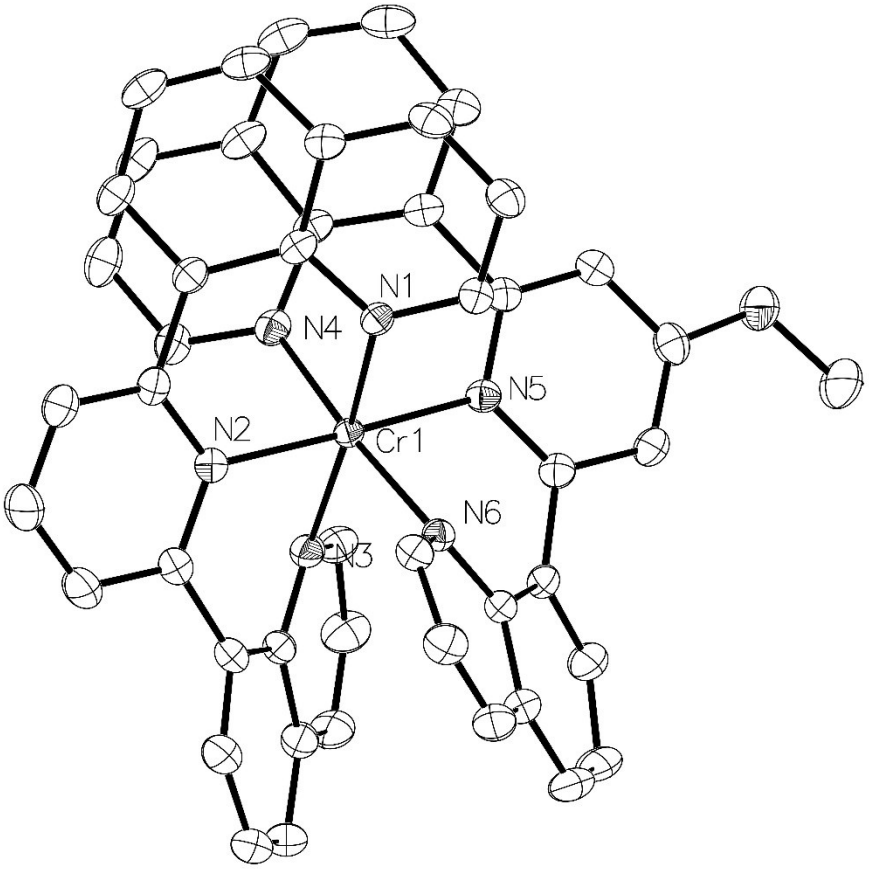

Figure S5 ORTEP view of [Cr(dqp)(dqpOMe)]$(CF_3SO_3)_3$ (**3**) with numbering scheme. Thermal ellipsoids are drawn at 50% probability level. Counter ions and H atoms are omitted for clarity.

Table S13. Selected transitions of absorption spectra recorded for **1, 2**, **3** in CH_3CN at 10^{-4} M between 250-650 nm and at *circa* 1 mM between 650-850 nm at 293 K.

Compound	λ (nm)	ν (cm^{-1})	ε ($M^{-1}\,cm^{-1}$)	Assignment
$[Cr(dqp)(tpy)]^{3+}$	280	35741	29589	π*← π
	311	32154	26153	π*← π
	358	27932	12032	π*← π
	400	25062	4875	LMCT/(MC)
	472	21186	634	$^4T_2$←$^4A_2$
	680	14705	0.08	$^2T_1'''(C_2)$←$^4A_2'(C_2)$
	698	14326	0.18	$^2T_1''(C_2)$←$^4A_2'(C_2)$
	725	13779	0.04	$^2T_1'(C_2)$←$^4A_2'(C_2)$
	736	13586	0.11	$^2E''(C_2)$←$^4A_2'(C_2)$
	749	13351	0.15	$^2E'(C_2)$←$^4A_2'(C_2)$
$[Cr(ddpd)(dqp)]^{3+}$	278	35971	32589	π*← π
	323	30959	41616	π*← π
	362	27624	28173	π*← π
	395	25316	21015	π*← π
	415	24096	[a]	$^4T_2$←$^4A_2$
	453	22075	3221	LMCT/(MC)
	696	14367	0.15	$^2T_1'''(C_2)$←$^4A_2(C_2)$
	719	13908	0.07	$^2T_1''(C_2)$←$^4A_2(C_2)$
	732	13661	0.30	$^2T_1'(C_2)$←$^4A_2(C_2)$
	763	13097	0.23	$^2E'(C_2)$←$^4A_2(C_2)$
$[Cr(dqp)(dqpOMe)]^{3+}$	334	29940	34427	π*← π
	374	26737	30974	π*← π
	409	24449	[a]	$^4T_2$←$^4A_2$
	467	21413	700	LMCT/(MC)
	698	14326	0.093	$^2T_1''(C_2)$←$^4A_2(C_2)$
	727	13755	0.34	$^2T_1'(C_2)$←$^4A_2(C_2)$
	753	13280	0.06	$^2E'(C_2)$←$^4A_2(C_2)$

[a] Not given because of the overlap with LMCT

Table S14. Energies of the Cr($^4A_2$), Cr($^2T_1$) and Cr(^2E) levels and ligand field Δ and Racah parameters B and C computed with eqs S1-S3 for $[Cr(dqp)(tpy)]^{3+}$ (1) $[Cr(ddpd)(dqp)]^{3+}$ (2) and $[Cr(dqp)(dqpOMe)]^{3+}$ in acetonitrile solution at 293 K.

Racah parameters B and C have been estimated with the help of eqs S1-S3.[S8-S10]

$E(^4T_2) = \Delta$ (S1)

$E(^2T_1) = 9B + 3C - 24(B^2/\Delta)$ (S2)

$E(^2E) = 9B + 3C - 50(B^2/\Delta)$ (S3)

Compound	Δ /cm^{-1}	B /cm^{-1}	C /cm^{-1}	Δ/B	C/B	$^2T_2$ /cm^{-1} [b]	$^4T_1$ /cm^{-1} [b]	Reference
1	21186	811	2571	26	3.2	*19756*	*33896*	This work
2	24096	779	2492	31	3.2	*20490*	*32077*	This work
3	24449	784	2509	31	3.2	*20626*	*31193*	This work
$[Cr(dqp)_2]^{3+}$	24937	656	2791	38	4.3	*20758*	*32030*	S11
$[Cr(ddpd)_2]^{3+}$ [b]	22883	763	2442	30	3.2	*19176*	*30828*	S11

[a] The energy of Cr($^2T_1$) is taken as the average of its split components (see text). [b] Computed using $E(^2T_2) = 15B + 5C - 176(B^2/\Delta)$ and $E(^4T_1) = 1.5\Delta + 7.5B - 0.5\sqrt{225B^2 + \Delta^2 - 18\Delta B}$.[S8, S9] [b] In water.

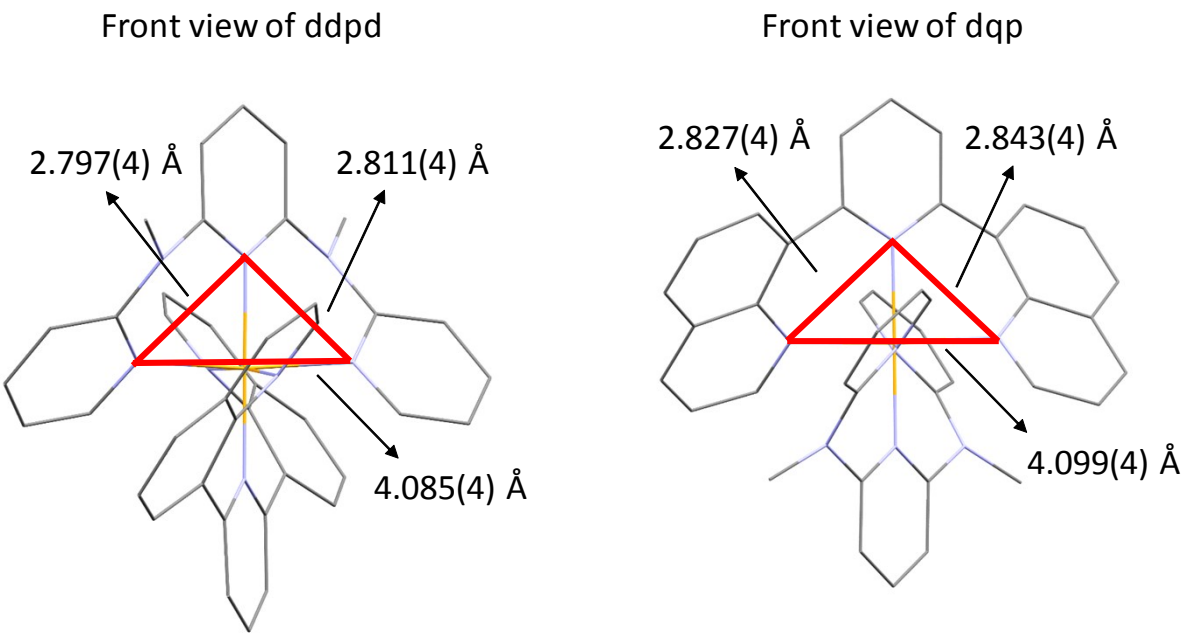

Figure S6. Calculated N(terminal)-N(central) and N(terminal)-N(terminal) distances for the bound ddpd (left) and (dqp) right in compound **2**.

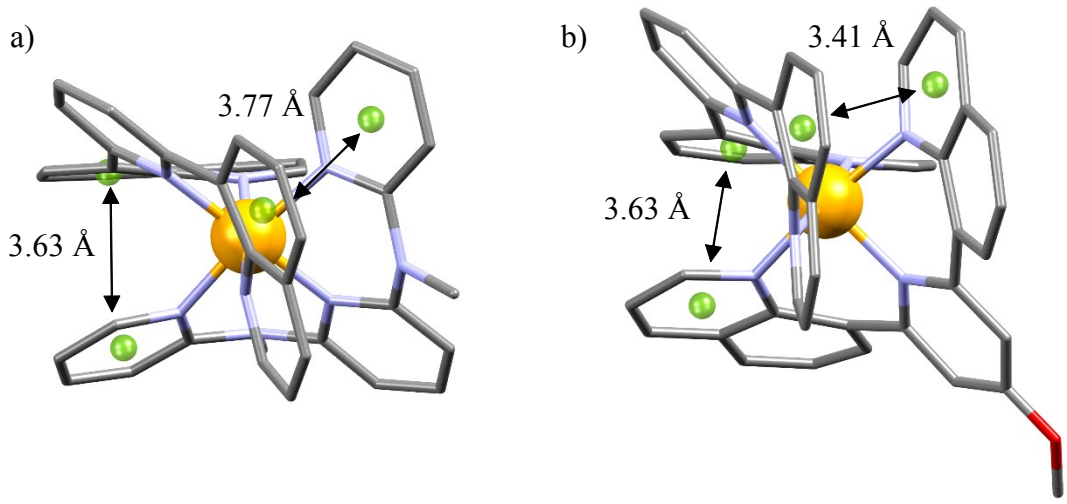

Figure S7. (a) Intramolecular interstrand π-stacking occurring between the quinoline rings and the amino-pyridine rings in **2** and (b) intramolecular interstrand stacking through π interaction involving quinoline rings in **3**. Colour code for the atoms: C (gray), N (blue), O(red) and Cr (orange). The centroids of the staked aromatic planes are represented with green spheres.

a)

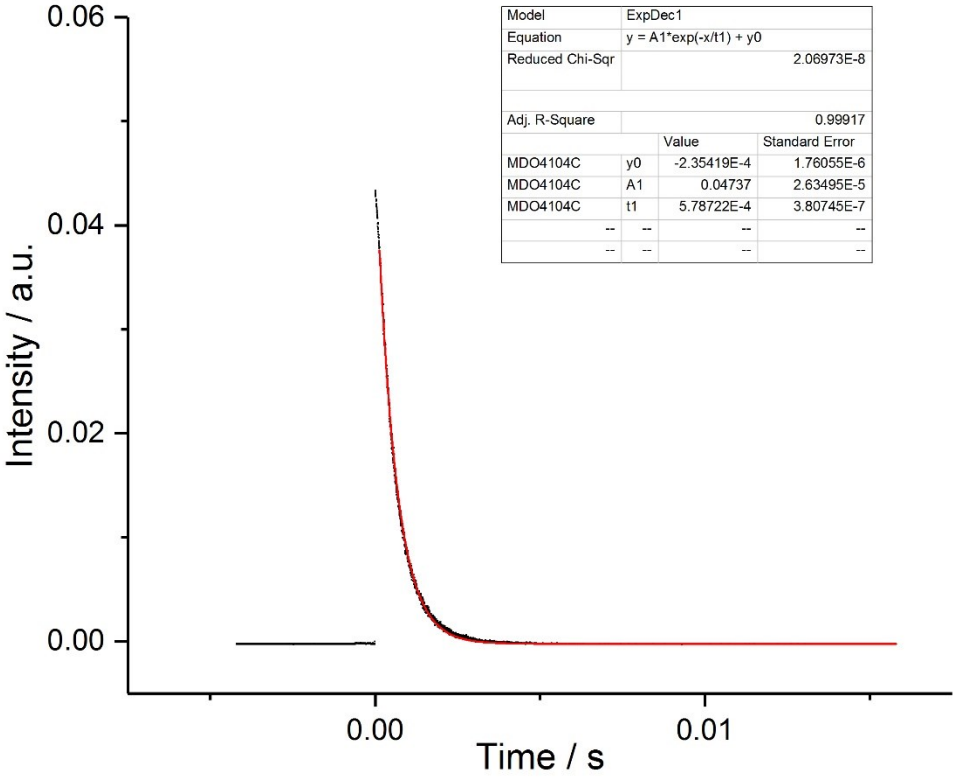
Model ExpDec1
Equation y = A1*exp(-x/t1) + y0
Reduced Chi-Sqr 2.06973E-8
Adj. R-Square 0.99917
Value Standard Error
MDO4104C y0 -2.35419E-4 1.76055E-6
MDO4104C A1 0.04737 2.63495E-5
MDO4104C t1 5.78722E-4 3.80745E-7
0.06
0.04
0.02
0.00
Intensity / a.u.
0.00
0.01
Time / s

b)

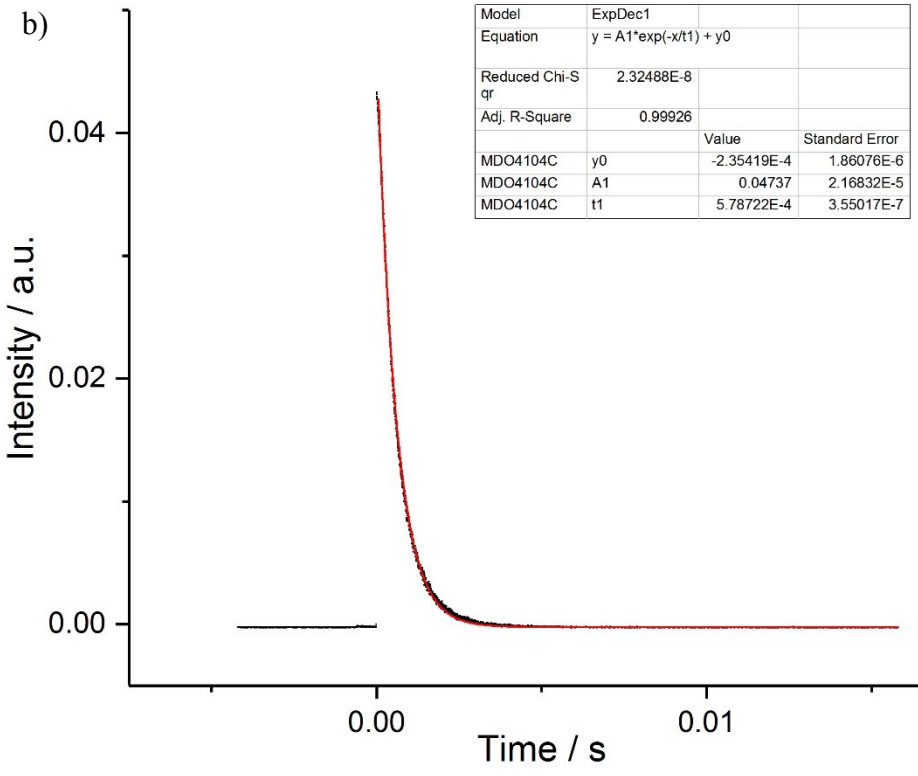
Model ExpDec1
Equation y = A1*exp(-x/t1) + y0
Reduced Chi-Sqr 2.32488E-8
Adj. R-Square 0.99926
Value Standard Error
MDO4104C y0 -2.35419E-4 1.86076E-6
MDO4104C A1 0.04737 2.16832E-5
MDO4104C t1 5.78722E-4 3.55017E-7
0.04
0.02
0.00
Intensity / a.u.
0.00
0.01
Time / s

b

c)

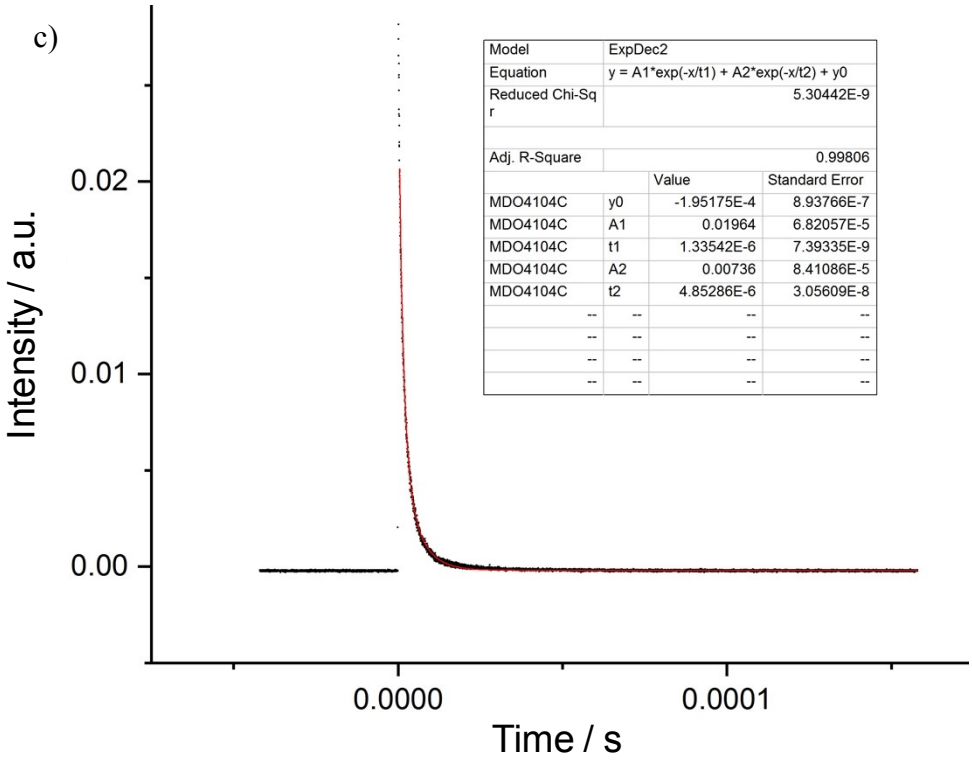

Model	ExpDec2		
Equation	y = A1*exp(-x/t1) + A2*exp(-x/t2) + y0		
Reduced Chi-Sqr			5.30442E-9
Adj. R-Square			0.99806
		Value	Standard Error
MDO4104C	y0	-1.95175E-4	8.93766E-7
MDO4104C	A1	0.01964	6.82057E-5
MDO4104C	t1	1.33542E-6	7.39335E-9
MDO4104C	A2	0.00736	8.41086E-5
MDO4104C	t2	4.85286E-6	3.05609E-8
--	--	--	--
--	--	--	--
--	--	--	--
--	--	--	--

d)

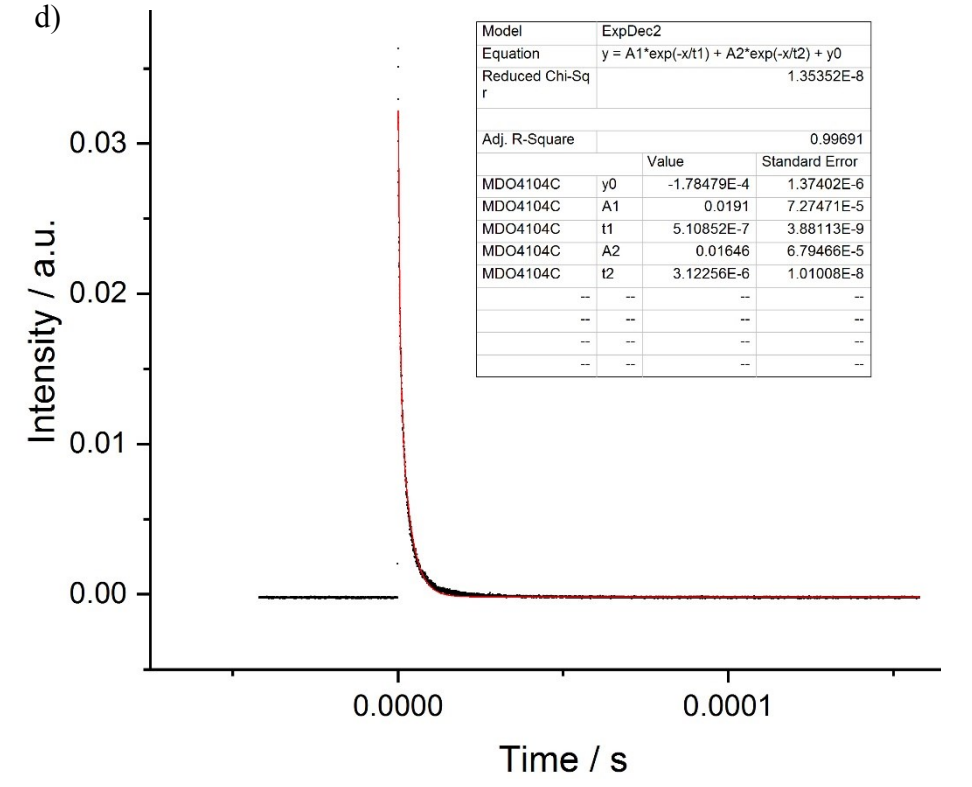

Model	ExpDec2		
Equation	y = A1*exp(-x/t1) + A2*exp(-x/t2) + y0		
Reduced Chi-Sqr			1.35352E-8
Adj. R-Square			0.99691
		Value	Standard Error
MDO4104C	y0	-1.78479E-4	1.37402E-6
MDO4104C	A1	0.0191	7.27471E-5
MDO4104C	t1	5.10852E-7	3.88113E-9
MDO4104C	A2	0.01646	6.79466E-5
MDO4104C	t2	3.12256E-6	1.01008E-8
--	--	--	--
--	--	--	--
--	--	--	--
--	--	--	--

e)

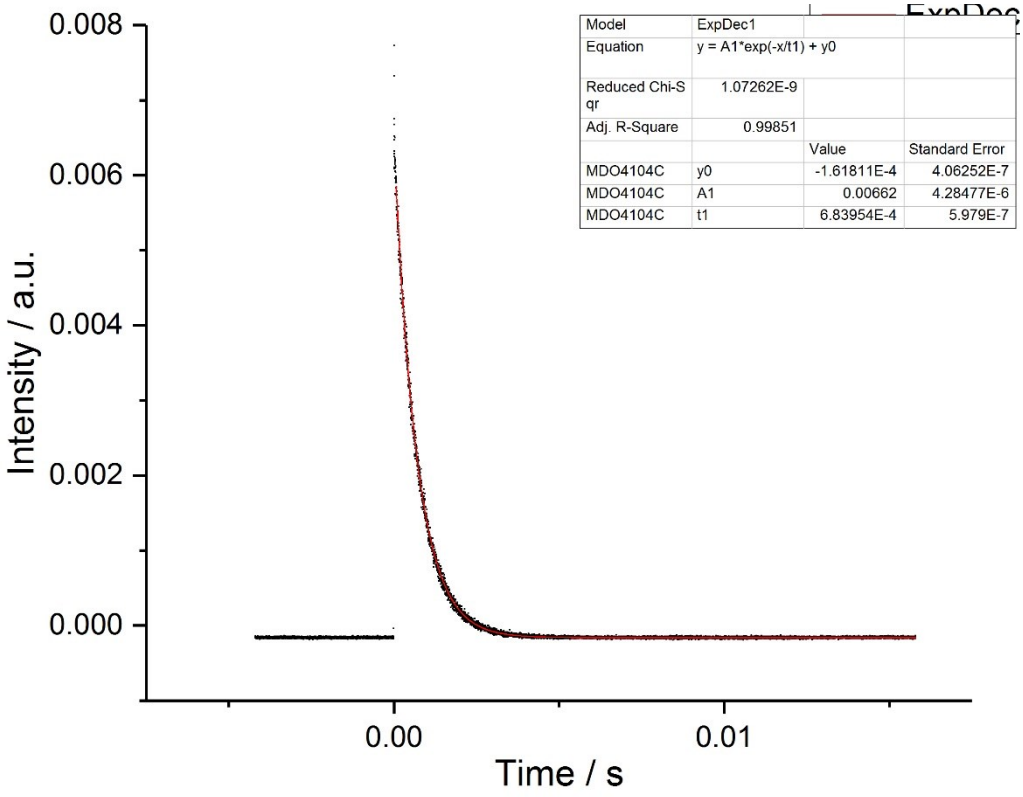
ExpDec
Model ExpDec1
Equation y = A1*exp(-x/t1) + y0
Reduced Chi-Sqr 1.07262E-9
Adj. R-Square 0.99851
Value Standard Error
MDO4104C y0 -1.61811E-4 4.06252E-7
MDO4104C A1 0.00662 4.28477E-6
MDO4104C t1 6.83954E-4 5.979E-7
0.008
0.006
0.004
0.002
0.000
Intensity / a.u.
0.00
0.01
Time / s

f)

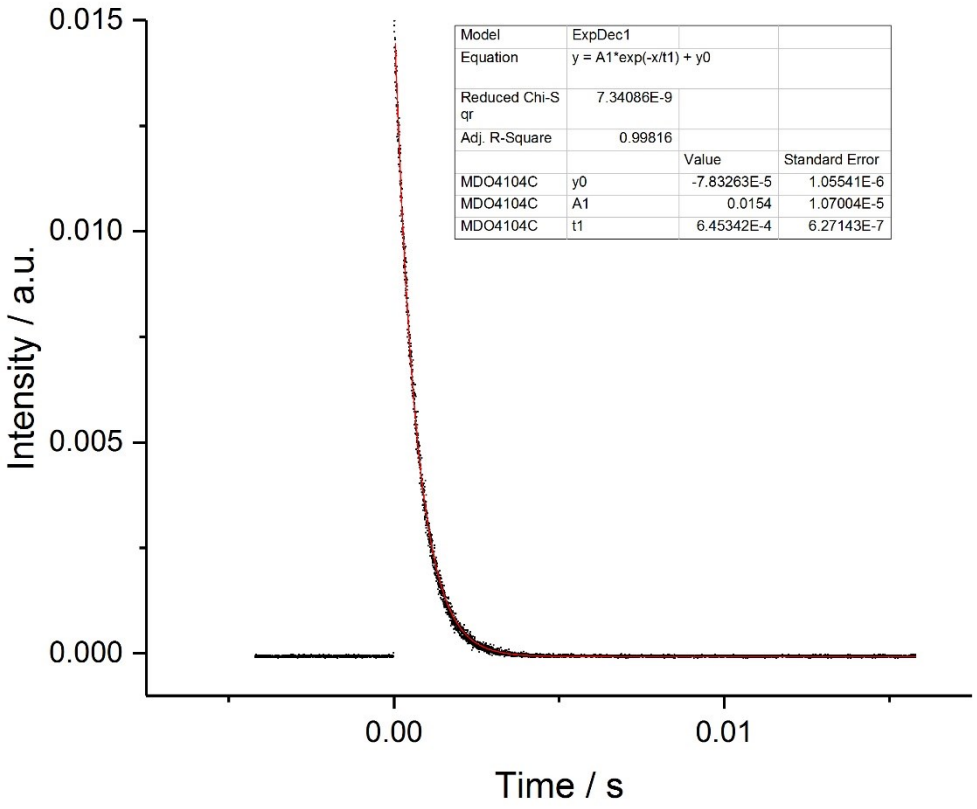
Model ExpDec1
Equation y = A1*exp(-x/t1) + y0
Reduced Chi-Sqr 7.34086E-9
Adj. R-Square 0.99816
Value Standard Error
MDO4104C y0 -7.83263E-5 1.05541E-6
MDO4104C A1 0.0154 1.07004E-5
MDO4104C t1 6.45342E-4 6.27143E-7
Intensity / a.u.
0.015
0.010
0.005
0.000
0.00
0.01
Time / s

g)

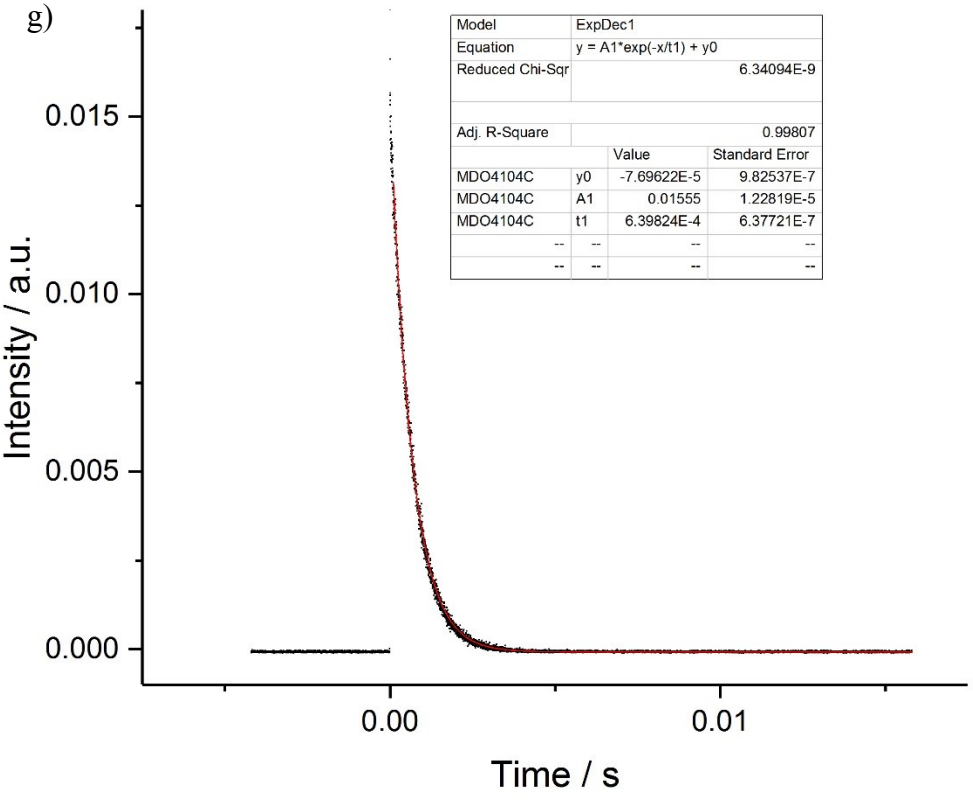
Model ExpDec1
Equation y = A1*exp(-x/t1) + y0
Reduced Chi-Sqr 6.34094E-9
Adj. R-Square 0.99807
Value Standard Error
MDO4104C y0 -7.69622E-5 9.82537E-7
MDO4104C A1 0.01555 1.22819E-5
MDO4104C t1 6.39824E-4 6.37721E-7
Intensity / a.u.
0.015
0.010
0.005
0.000
0.00
0.01
Time / s

h)

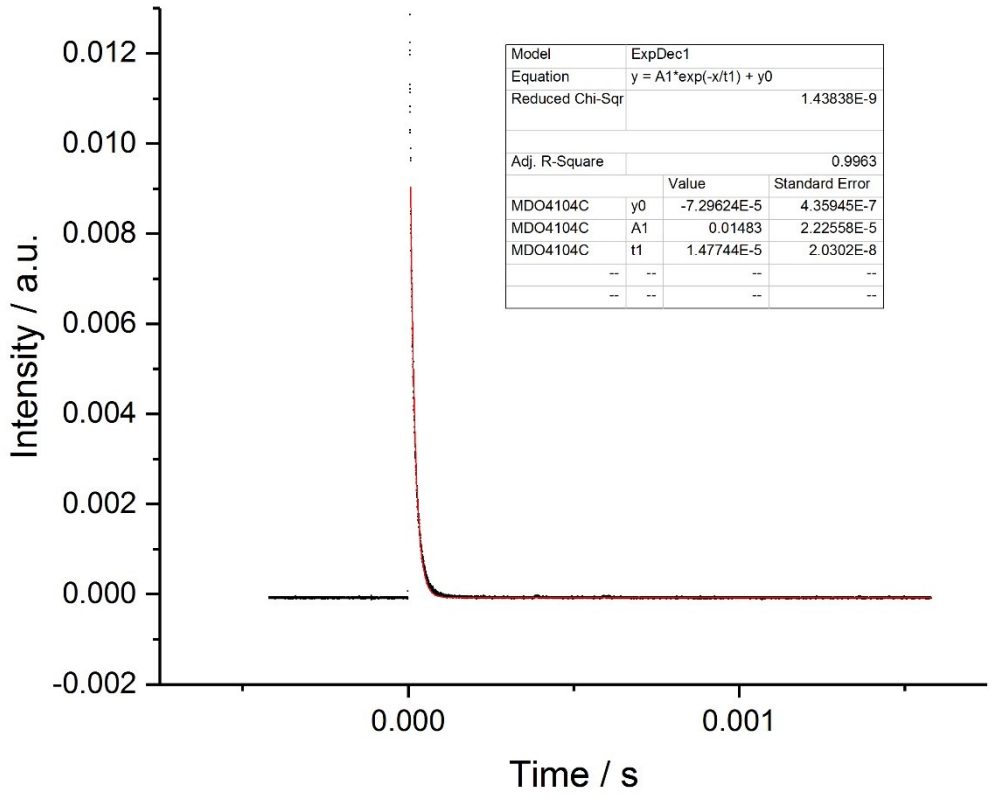
Model ExpDec1
Equation y = A1*exp(-x/t1) + y0
Reduced Chi-Sqr 1.43838E-9
Adj. R-Square 0.9963
Value Standard Error
MDO4104C y0 -7.29624E-5 4.35945E-7
MDO4104C A1 0.01483 2.22558E-5
MDO4104C t1 1.47744E-5 2.0302E-8
0.012
0.010
0.008
0.006
0.004
0.002
0.000
-0.002
Intensity / a.u.
0.000
0.001
Time / s

i)

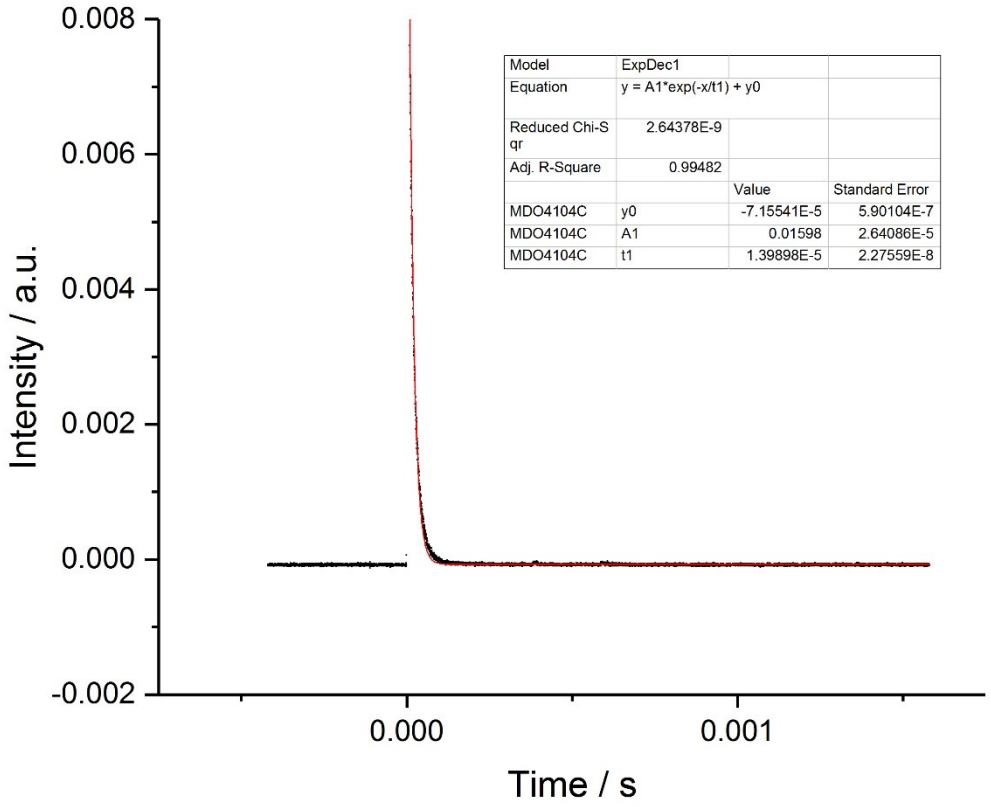
Model ExpDec1
Equation y = A1*exp(-x/t1) + y0
Reduced Chi-Sqr 2.64378E-9
Adj. R-Square 0.99482
Value Standard Error
MDO4104C y0 -7.15541E-5 5.90104E-7
MDO4104C A1 0.01598 2.64086E-5
MDO4104C t1 1.39898E-5 2.27559E-8
0.008
0.006
0.004
0.002
0.000
-0.002
Intensity / a.u.
0.000
0.001
Time / s

j)

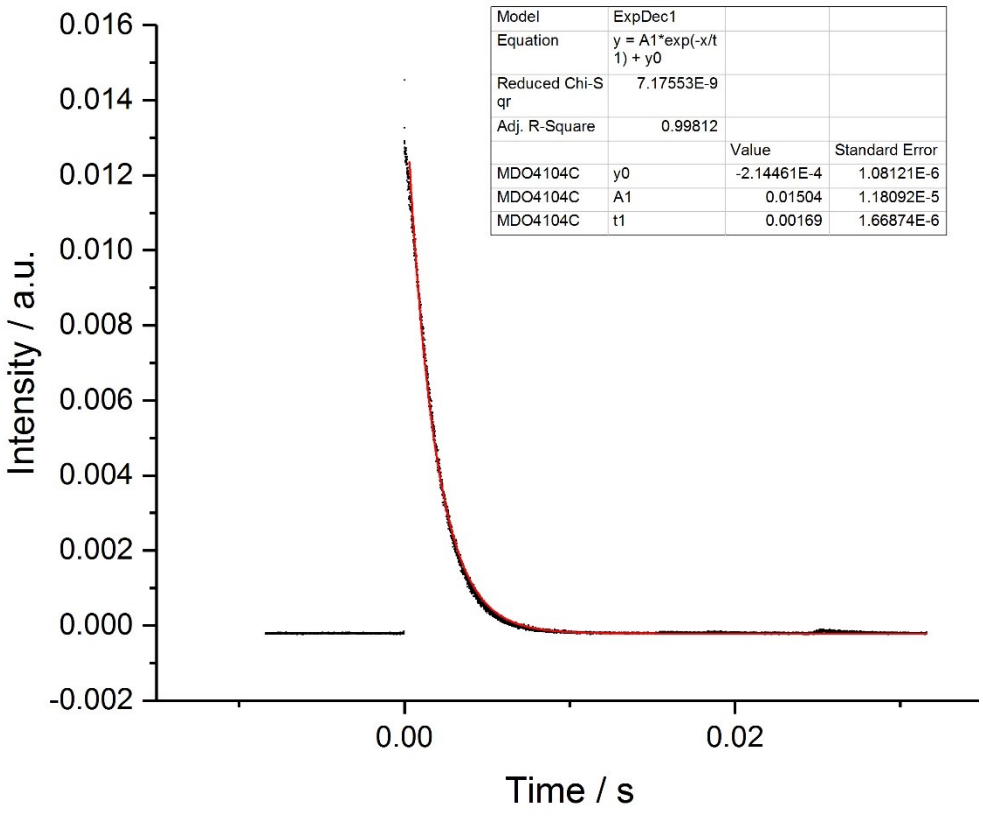
Model ExpDec1
Equation y = A1*exp(-x/t1) + y0
Reduced Chi-Sqr 7.17553E-9
Adj. R-Square 0.99812
Value Standard Error
MDO4104C y0 -2.14461E-4 1.08121E-6
MDO4104C A1 0.01504 1.18092E-5
MDO4104C t1 0.00169 1.66874E-6
Intensity / a.u.
0.016
0.014
0.012
0.010
0.008
0.006
0.004
0.002
0.000
-0.002
0.00
0.02
Time / s

k)

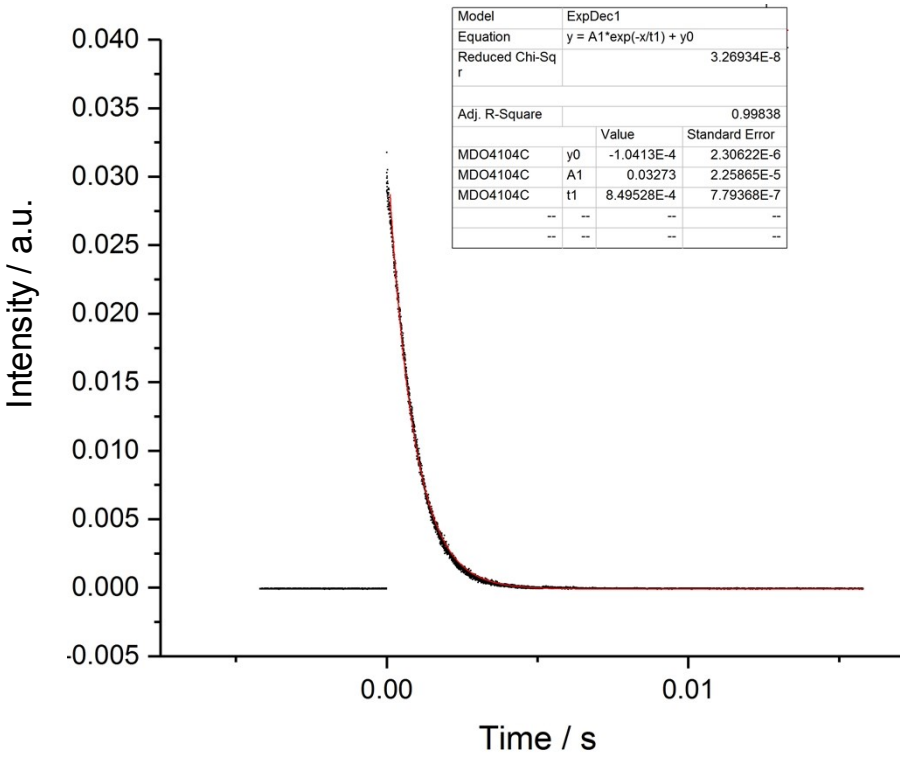
Model ExpDec1
Equation y = A1*exp(-x/t1) + y0
Reduced Chi-Sqr 3.26934E-8
Adj. R-Square 0.99838
Value Standard Error
MDO4104C y0 -1.0413E-4 2.30622E-6
MDO4104C A1 0.03273 2.25865E-5
MDO4104C t1 8.49528E-4 7.79368E-7
0.040
0.035
0.030
0.025
0.020
0.015
0.010
0.005
0.000
-0.005
Intensity / a.u.
0.00
0.01
Time / s

l)

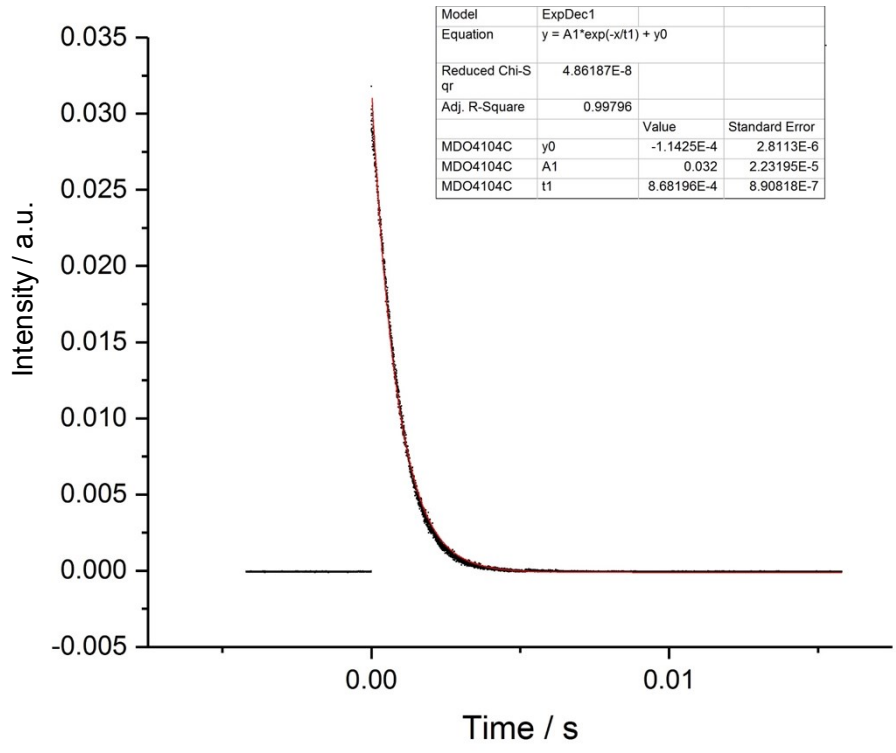
Model ExpDec1
Equation y = A1*exp(-x/t1) + y0
Reduced Chi-Sqr 4.86187E-8
Adj. R-Square 0.99796
Value Standard Error
MDO4104C y0 -1.1425E-4 2.8113E-6
MDO4104C A1 0.032 2.23195E-5
MDO4104C t1 8.68196E-4 8.90818E-7
0.035
0.030
0.025
0.020
0.015
0.010
0.005
0.000
-0.005
Intensity / a.u.
0.00
0.01
Time / s

m)

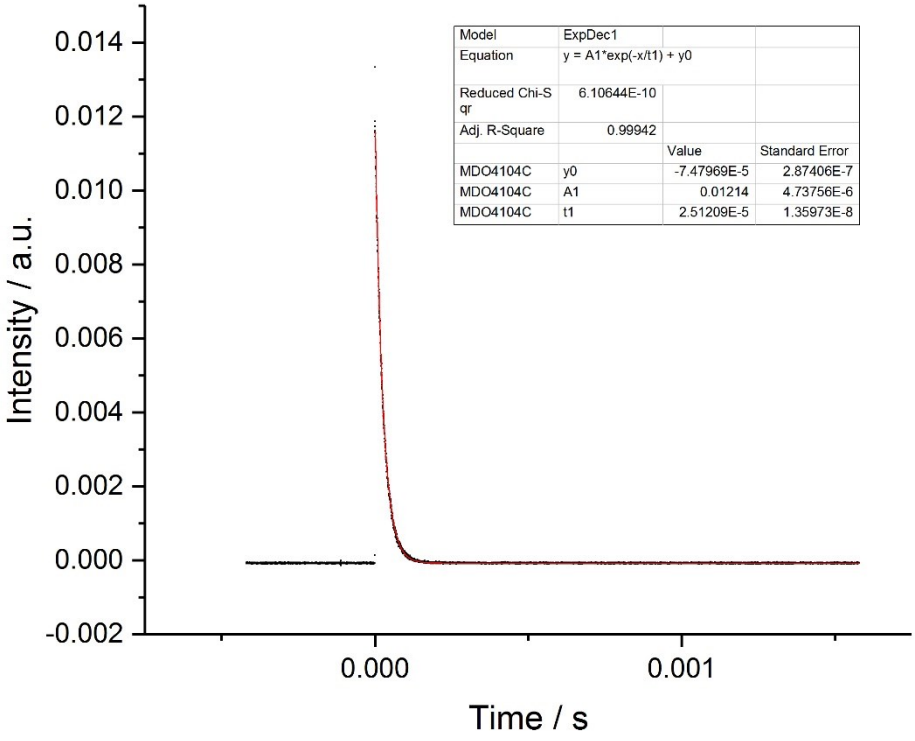
Model ExpDec1
Equation y = A1*exp(-x/t1) + y0
Reduced Chi-Sqr 6.10644E-10
Adj. R-Square 0.99942
Value Standard Error
MDO4104C y0 -7.47969E-5 2.87406E-7
MDO4104C A1 0.01214 4.73756E-6
MDO4104C t1 2.51209E-5 1.35973E-8
Intensity / a.u.
0.014
0.012
0.010
0.008
0.006
0.004
0.002
0.000
-0.002
0.000
0.001
Time / s

n)

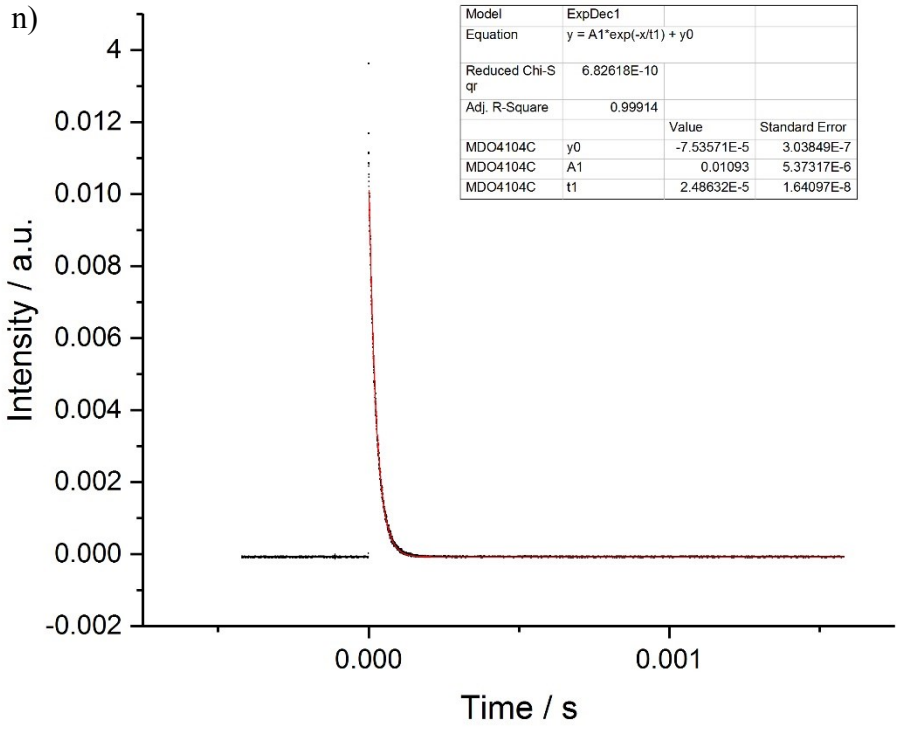
Model ExpDec1
Equation y = A1*exp(-x/t1) + y0
Reduced Chi-Sqr 6.82618E-10
Adj. R-Square 0.99914
Value Standard Error
MDO4104C y0 -7.53571E-5 3.03849E-7
MDO4104C A1 0.01093 5.37317E-6
MDO4104C t1 2.48632E-5 1.64097E-8
Intensity / a.u.
4
0.012
0.010
0.008
0.006
0.004
0.002
0.000
-0.002
0.000
0.001
Time / s

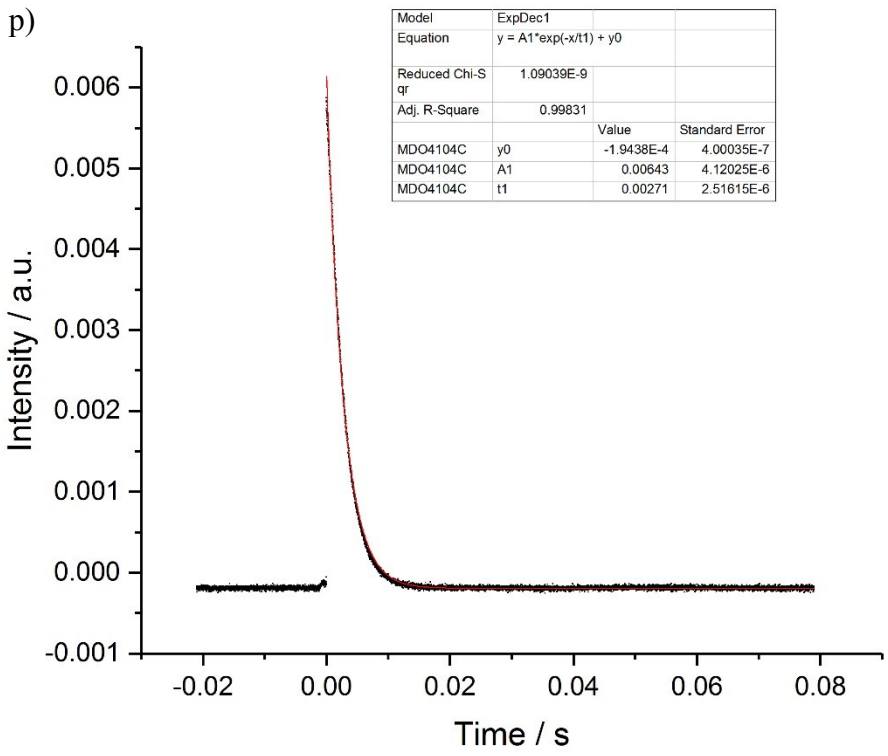

Figure S8. Excited state lifetime fitting for the series of heteroleptic complexes (λ_{exc} = 355 nm): a) and b) Cr(^{2}E) and Cr(^{2}T$_1$) lifetimes for **1** in deaerated acetonitrile solution; c) and d) Cr(^{2}E) and Cr(^{2}T$_1$) lifetimes for **1** in aerated acetonitrile solution and e) Cr(^{2}E) lifetime for **1** at 77 K in frozen acetonitrile /propionitrile (6/4) solution. f) and g) Cr(^{2}E) and Cr(^{2}T$_1$) lifetimes for **2** in deaerated acetonitrile solution; h) and i) Cr(^{2}E) and Cr(^{2}T$_1$) lifetimes for **2** in aerated acetonitrile solution and j) Cr(^{2}E) lifetime for **2** at 77 K in frozen acetonitrile /propionitrile (6/4) solution. k) and l) Cr(^{2}E) and Cr(^{2}T$_1$) lifetimes for **3** in deaerated acetonitrile solution; m) and n) Cr(^{2}E) and Cr(^{2}T$_1$) lifetimes for **3** in aerated acetonitrile solution and p) Cr(^{2}E) lifetime for **3** at 77 K in frozen acetonitrile /propionitrile (6/4) solution.

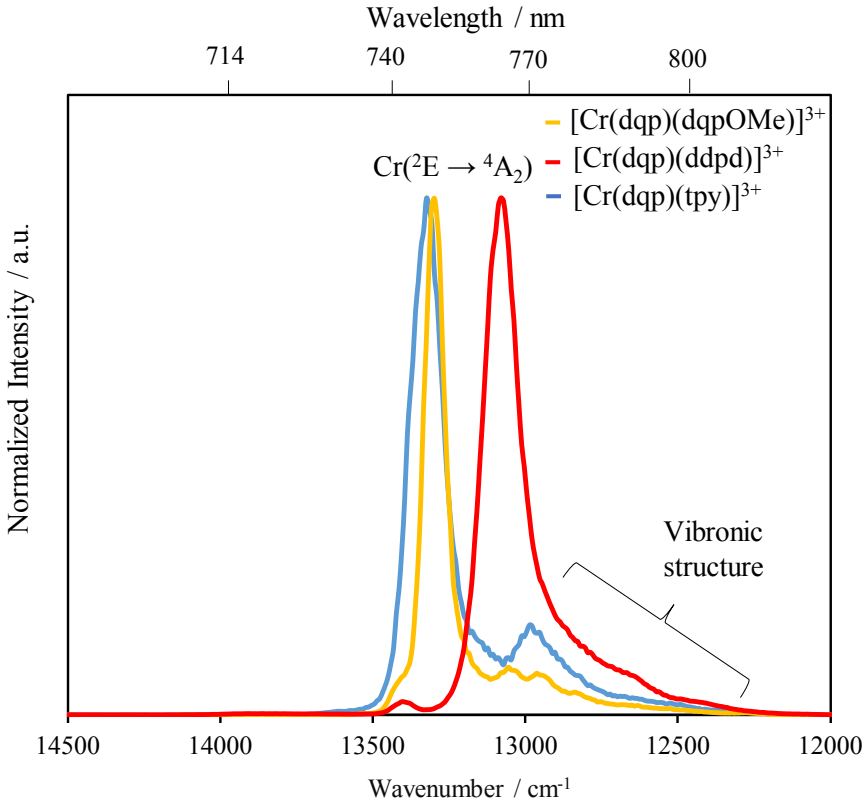

Figure S9. Emission spectra at 77 K in frozen acetonitrile /propionitrile (6/4) solution

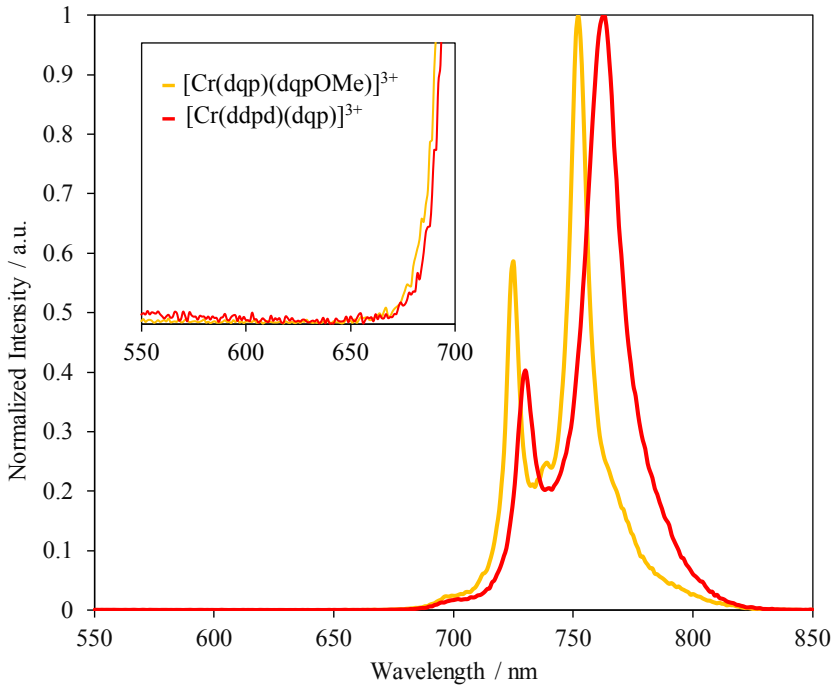

Figure S10. Emission spectra at room temperature in acetonitrile solution from 550 to 850 nm

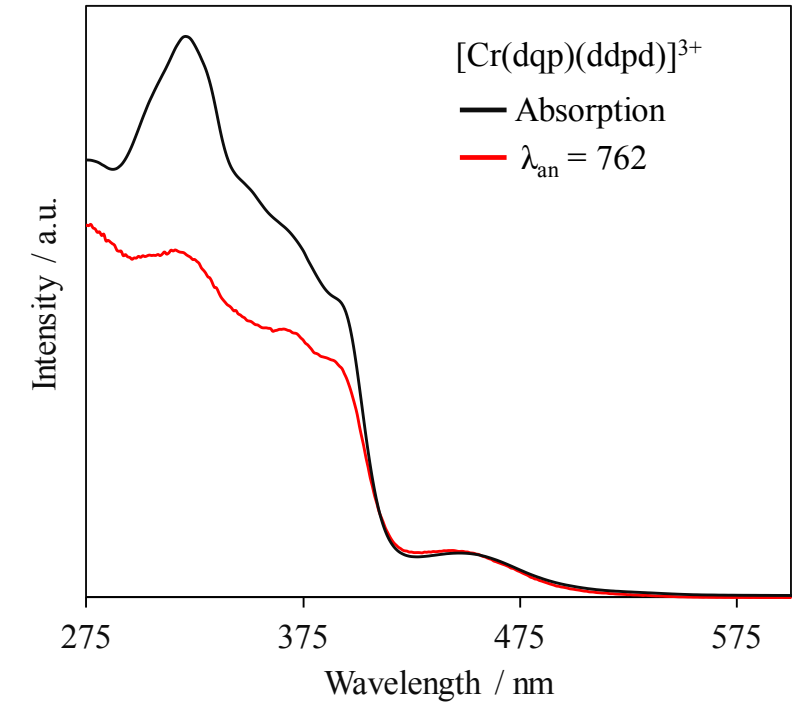

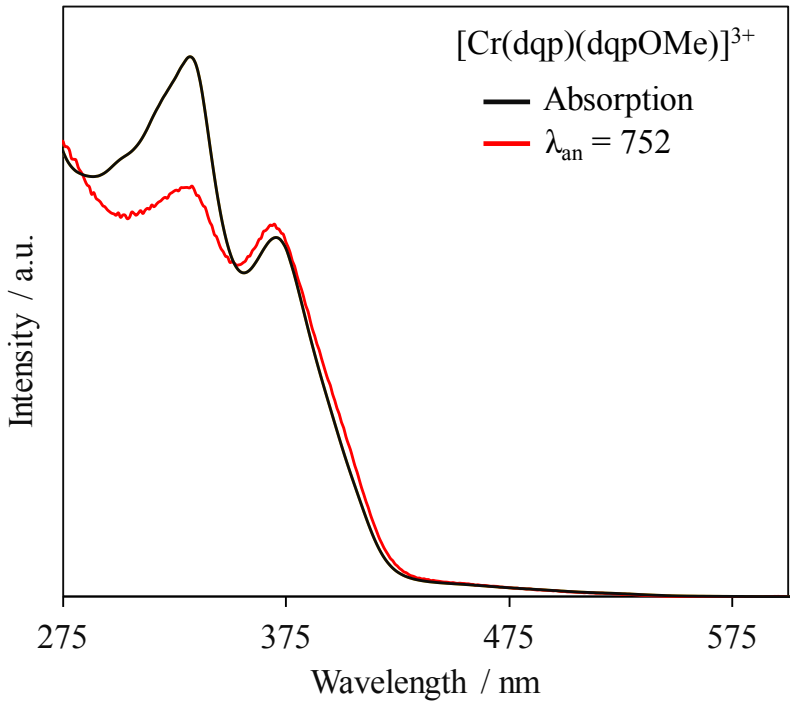

Figure S11. Excitation spectra of compounds **2** and **3** at λ_{an} = 762 nm and λ_{an} = 752 respectively in CH_3CN solution.

Table S15. Kinetic rate constants and emission quantum yields recorded for **1**, **2** and **3** in acetonitrile and $[Cr(dqp)_2]^{3+}$ in water[S8] at 293 K and 77K. Values in italic type represents the values obtained for aerated solutions, the rest for deaerated solutions.

	$k_{Cr,rad}^{^2E}$ [a] /s^{-1}	$k_{Cr,rad}^{^2T_1}$ [a] /s^{-1}	$k_{Cr,nrad}^{^2E}$ [b] /s^{-1}	$k_{Cr,nrad}^{^2T_1}$ [b] /s^{-1}	$\tau_{Cr,obs}^{^2E,\,^2T_1}$ [c] /μs	$\tau_{Cr,obs}^{^2E,\,^2T_1}$ [d] /μs	$\tau_{Cr,obs}^{^2E,\,^2T_1}$ [e] /ms	$\Phi_{Cr}^{Cr(^2E)}$ [f] /%	$\Phi_{Cr}^{Cr(^2T_1)}$ [g] /%	Φ_{Cr}^{L} [h] /%	Φ_{Cr}^{L} [i] /%	$\eta_{sens}^{L\rightarrow Cr}$ [j] /%
1	55(5)	58(5)	1699(30)	1696(30)	578(10)	*3.0(1)*	0.7(1)	3.2(3)	3.4(3)	0.2(1)	*0.0015(1)*	3.0(5)
2	63(6)	91(8)	1500(30)	1472(30)	642(10)	*14(2)*	1.7(2)	4.0(4)	5.8(5)	6.0(5)	*0.12(1)*	61(5)
3	11(1)	62(6)	1139(20)	1088(20)	855(10)	*25(2)*	2.7(2)	0.9(1)	5.3(1)	6.5(5)	*0.16(2)*	100(7)
$[Cr(dqp)_2]^{3+}$ [k]	30(2)	89(5)	803(15)	744(15)	1200(20)	*83(5)*	3.1(2)	3.6(1)	11.0(1)	7.3(4)	*1.0(1)*	50(7)

[a] k_{rad} obtained from $k_{rad} = 2303 \times \frac{8\pi c n^2 \tilde{\nu}^2 g_{G.S.}}{N_A g_{E.E.}} \int \varepsilon(\tilde{\nu}) d\tilde{\nu}$ where c is the velocity of the light in vacuum, N_A is Avogrado's number, n is the refractive index of the medium, $\tilde{\nu}$ is the transition wavenumber, ε is the molar absorption coefficient, $g_{G.S.}$ is the degeneracy of the ground state ($g(^4A_2) = 4$) and $g_{E.E.}$ represents the degeneracy of the excited states ($g(^2E) = 4$ and $g(^2T_1) = 6$).[3] [b] $k_{nrad} = (1/\tau_{obs}) - k_{rad}$ (deaerated solution). [c] τ_{obs} from time-resolved experiments at 293K (deaerated solution). [d] τ_{obs} from time-resolved experiments at 293K (aerated solution). [e] τ_{obs} from time-resolved experiments at 77K. [f,g] Intrinsic quantum yield of the specified Cr level calculated with $\Phi_{Cr}^{Cr} = k_{rad}\,\tau_{obs.}$(deaerated solutions). [h,i] Overall quantum yield Φ_{Cr}^{L} measured by relative method using $[Cr(ddpd)_2]^{3+}$ (λ_{exc} = 435 nm in H_2O; Φ_{Cr}^{L} = 11%) in [h]deaerated and [i]aerated solutions. [j] $\eta_{sens}^{L\rightarrow Cr} = \frac{\Phi_{Cr}^{L}}{\Phi_{Cr}^{Cr(^2E)} + \Phi_{Cr}^{Cr(^2T_1)}}$ (deaerated solution). Lifetime: estimated relative uncertainty □ 10%. Quantum yield: estimated relative uncertainty □10%. [k] Recalculated from ref. S8.

References

(S1) S. Otto, M. Grabolle, C. Förster, C. Kreitner, U. Resch-Genger and K. Heinze, *Angew. Chem., Int. Ed.*, 2015, **54**, 11572–11576.

(S2) M. Jäger, R.-J. Kumar, H. Görls H., J. Bergquist J. and O. Johansson. *Inorg. Chem*. 2009, **48**, 3228-3238

(S3) G. Angulo, G. Grampp and A. Rosspeintner, *Spectrochim. Acta Part a-Molecular and Biomolecular Spectroscopy* 2006, **65**, 727-731.

(S4) H. Ishida, J.-C. G. Bünzli and A. Beeby, *Pure Appl. Chem*., 2016, **7**, 88

(S5) G. M. Sheldrick. SHELXT - Integrated Space-group and Crystal-structure Determination. *Acta Cryst. A* 2015, **71**, 3–8.

(S6) G. M. Sheldrick. Crystal Structure Refinement with SHELXL. *Acta Cryst. C*, 2015, **71**, 3–8.

(S7) O. V. Dolomanov, L. J. Bourhis, R. J. Gildea, J. A. K. Howard and H. Puschmann, *J Appl. Cryst*. 2009, **42**, 339–341.

(S8) C. K. Jorgensen, Adv. Chem. Phys., 1963, 5, 33–146.

(S9) A. B. P. Lever, Inorg. Electron. Spectrosc. Elsevier, Amsterdam, Oxford, New York, Tokyo, 2nd edn, 1984, 126.

(S10) D. Zare, B. Doistau, H. Nozary, C. Besnard, L. Guénée, Y. Suffren, A.-L. Pelé, A. Hauser and C. Piguet, *Dalton Trans.*, 2017, **46**, 8992-9009.

(S11) J.-R Jiménez, B. Doistau, C. M. Cruz, C. Besnard, J. M. Cuerva, A. G. Campaña and C. Piguet. *J. Am. Chem. Soc.* 2019, **141**, 13244−13252.